

# Defocus test and defocus correction in full-field optical coherence tomography

S. Labiau<sup>1,2</sup>, G. David<sup>1,2</sup>, S. Gigan<sup>1,\*</sup>, A.C. Boccara<sup>1</sup>

<sup>1</sup> Institut Langevin, ESPCI, CNRS UMR 7587, Laboratoire d'Optique Physique, 10 rue Vauquelin, 75231 Paris Cedex 05, France.

<sup>2</sup> LLTech, Bio-incubateur Eurosanté, 70 rue du Dr. Yersin, 59120 LOOS - France

\*Corresponding author: [sylvain.gigan@espci.fr](mailto:sylvain.gigan@espci.fr)

We report experimental evidence and correction of defocus in full-field OCT of biological samples due to mismatch of the refractive index in biological tissues with regard to water. Via a metric based on the image quality, we demonstrate that we are able to compensate this index-induced defocus and to recover a sharp image in depth.

© 2022 Optical Society of America

Optical Coherence Tomography (OCT) [1] is a powerful technique used to image through scattering media by interferometric selection of ballistic photons. It has proven to be an invaluable tool for biological imaging, in particular in the field of eye examination. Most of the other tissues exhibit a larger scattering cross-section and it is more difficult to get sharp images at large depths with cell size resolution. In contrast with time domain OCT or Fourier domain OCT, Full-Field OCT (FF-OCT) [2] directly takes "en face" images. The sample is displaced to move the focal plane at different depths below the surface and obtain a 3D tomographic image. FF-OCT is in principle able to operate with high lateral resolution using medium or large aperture microscope objectives: indeed we have used N.A. ranging from 0.3 to 0.8 with water immersion objectives providing a lateral resolution ranging from about  $1.5\mu m$  to  $0.5\mu m$  when using a central wavelength of  $0.75\mu m$ . In principle, as long as the refractive index of the sample is close to water refractive index there is no need for the large depth of field required for time domain, spectral, Fourier-domain or swept-source OCT. For these last methods the available depth range is of the order of the depth of field of the optics, therefore requiring low numerical aperture optics that limits the lateral resolution. For example, for a depth of field larger than two hundred  $\mu m$ , the N.A. has to be lower than 0.1, giving a lateral resolution larger than  $5\mu m$ . Nevertheless in all approaches the axial sectioning ability is linked to the coherence length of the light source. In FF-OCT it is not

only necessary that the optical path length of the reference arm be matched to the length of the sample arm, it is also crucial that both arms are as symmetric as possible in term of refractive indexes. As a consequence, FF-OCT generally uses water-immersion microscope objective, water being the main component of biological tissues. Nevertheless, the refractive index of tissues of medical interest ranges from 1.35 to more than 1.50 [4]. When focusing inside such tissues with a refractive index larger than  $n = 1.33$  (water) the focusing is shifted forward while the sectioning plane goes backward (figure 2). This phenomenon has been used previously to measure the refractive index of various tissues [4]. More precisely, in the paraxial approximation a displacement of the surface of  $z$  in a medium of refractive index  $n'$  (instead of  $n$ ) shifts the focusing forward by a distance

$$F(z) = \frac{n'}{n}z \quad (1)$$

while the zero path difference is shifted backward (larger refractive index) by

$$\Pi(z) = -\frac{n}{n'}z \quad (2)$$

In order to match the position of the focusing and of the zero path difference one must introduce a path difference on the reference channel of:

$$\delta_f(z) = 2n'(F(z) + \Pi(z)) = 2n'z\left(\frac{n'}{n} - \frac{n}{n'}\right) = 2z\frac{n'^2 - n^2}{n} \quad (3)$$

As long as  $\delta_f/2n$  is smaller than the depth of field there is no need to correct the path difference from the mismatch between the two arms of the Linnik interferometer. For instance as one can see on figure 1 with the 0.3 numerical aperture water immersion objectives the depth of field is about 16 micrometers.

The experimental setup is based on an interference microscope in the Linnik configuration, i.e., a bulk Michelson interferometer with identical microscope objectives -for this study: Olympus, 10x/0.3 W - in both arms. An halogen lamp with a stabilized DC power supply is used as a spatially and temporally incoherent light source. A low ( $\sim 2\%$  with water immersion microscope objectives) reflection surface is placed at the focal plane of the microscope objective of the reference arm in order to maximize the contrast. The object to be imaged is placed in the other arm of the interferometer under an identical water-immersion microscope objective. The numerical aperture of the microscope objectives is 0.3, providing a theoretical transverse (x-y) resolution of  $\sim 1.4\mu m$  at the mean wavelength  $\lambda_0 = 750nm$ . The image of the reference mirror and the image of the object are projected with an achromatic doublet lens onto a CCD camera (DALSA 1M15, 15 Hz, 12 bits digitization, and 1024x1024 pixels). Due to the source spectrum, to the spectral response of the CCD camera and the optical elements of the experimental setup, the useful wavelengths range from approximately 600

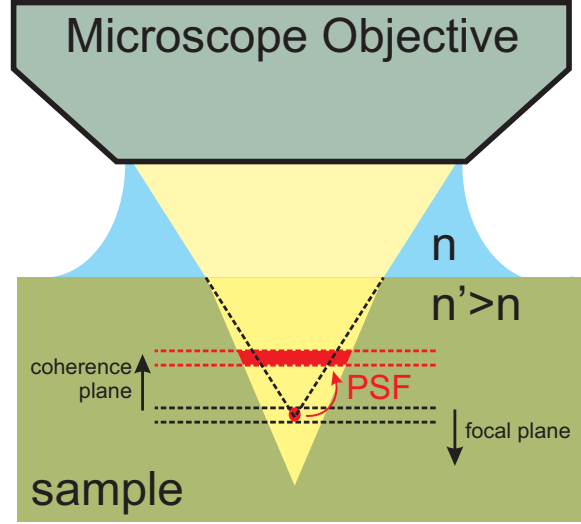


Fig. 1. principle of the defocusing phenomenon. in a tissue with index  $n'$  higher than water, the interference plane (corresponding to zero path difference) is shifted upwards while the focus is moves downwards.

nm to 900 nm giving an axial sectioning of less than  $1\mu m$ . To eliminate all the background signal and to keep only the interferometric signal the path difference is modulated by a PZT actuator. Data acquisition, camera control and PZT control are performed by a Visual C++ windows program.

To correct for defocus around a depth of interest for diagnostic for instance, we have adapted to our en face FF-OCT method an approach which has been proposed by Debarre et al. [3]. This approach relies on Fourier-Transform image analysis. In essence, the spatial frequency spectrum of an OCT image comprises several regions. The zero frequency region corresponds to the mean image intensity. The highest frequency region corresponds to noise from all origins (speckle, camera noise, photon noise). The intermediary frequency range corresponds mainly to the image itself, and contains all the informations about the sharp details. When defocus takes place, the amount of energy in this intermediary region decreases due to the loss of details induced by the broadening of the point spread function (PSF). As a metric of the focusing quality, we therefore monitored the total energy in the intermediary region of the Fourier-transformed image. This energy is maximum when the aberration is minimized. Around the optimal position, this metric show a well-behaved quadratic shape while farther from the optimum position we found it best fitted by a lorentzian. By adding a known aberration, we can try several values of the defocus (with a minimum of 3 measurements [3]) and measure the image quality for each of them. This way, we can reconstruct the metric shape, and infer the optimal position. Note that we only applied this criterion to

defocus (which is in our case the main source of aberration, way above the spherical aberration), but that this image-based optimization method can be used to correct for any kind of aberration, provided it is possible to add a known quantity to a single aberration mode (with a deformable mirror for instance).

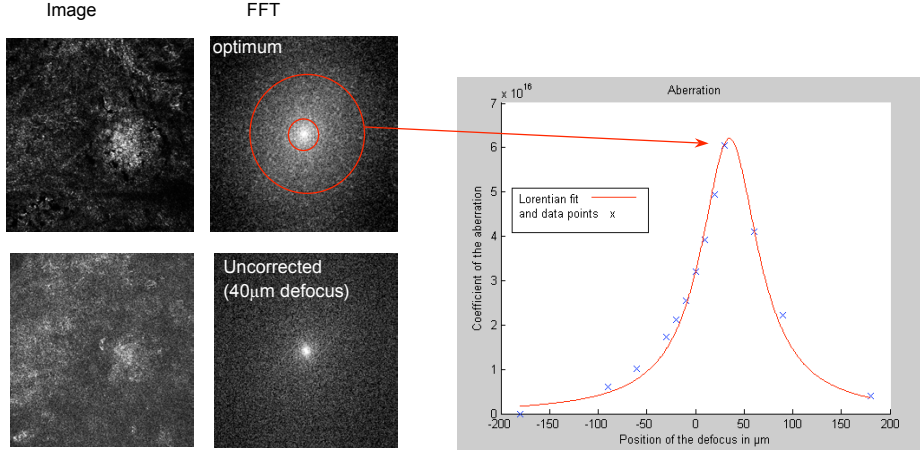


Fig. 2. Left: FF-OCT image and spatial spectrum FFT of the image for the uncorrected (lower) and optimal (upper) image. right: figure of merit as a function of defocus  $\delta z$  and Lorentzian Fit to obtain the optimal focus position. The sample is a sentinel lymph node, the width of the field of view is 500  $\mu m$ .

The experimental procedure was the following. The setup is pre-aligned by replacing the sample by a mirror and obtaining interferences with a maximized contrast: this first step insure focusing of both the reference and the sample arm, and that the two arms optical paths are matched in water, i.e, that the system is correctly aligned at the surface of the sample. We then move the sample towards the microscope objective, in order to image in-depth. In our experiment, we went up to  $200\mu m$  deep in a various tissues sample. Here we describe the results obtained with a sentinel lymph node. Since the index  $n'$  of the sample is larger than the index  $n$  of water, defocus starts to degrade the image quality. To try different values of the defocus in our system, we need to change the length of the reference arm in order to move the coherence sectionning plane relatively to the focus of the microscope objective. However, in order to use the metric, it is necessary to image always the same plane in the sample. We thus need, when changing the reference arm length by  $\delta z$  (in air), to move the sample in the same direction by a quantity  $\delta z/n'$ , so that the sectionning plane in the sample is unchanged.

For each position of the defocus, we acquired an image, and numerically Fast Fourier-transformed it. We determine manually the upper and lower frequencies of the integration

domain to maximise the signal-to-noise ratio. The results obtained are summarized in figure 2.  $z = 0$  corresponds to the length arm matched in water. We find that for our sample, at a depth  $z = 60\mu m$ , the optimum defocus is obtained for  $\delta_z \simeq 30\mu m$  (well above the depth of field of  $16\mu m$ ), and we see that we are able to recover much more signal, and much sharper details. Note that this allows us to directly estimate in-situ the refractive index of the sample, with a good accuracy. Here we find a value of  $n = 1.52 \pm 0.01$ , which is reasonable for such a dense tissue. We also see that even though the index mismatch is not large, as the OCT move out-of-focus linearly with the depth, the image quality is degraded very quickly, even for relatively low numerical aperture. Not taking this effect into account strongly limits the maximum imaging depth achievable in a given sample.

This wavefront correction of defocusing has proved to be efficient and simple to implement. This approach can be generalized to a stratified medium with a dependance of  $n'$  on depth, in particular the skin. For the first time an OCT image from a highly scattering sample has been corrected without wavefront analysis such as in [5] but only based on the optimization of the image quality. Compared to the results of [3] we have been able to correct an image captured well below the sample surface of highly scattering media. At this stage we still don't know if we have reached the optimum signal in term of resolution; it seems from the detailed analysis of cellular structure that we are close to this goal; nevertheless let us underline that this approach can be extended to other kinds of aberrations when coupled to a deformable mirror conjugated with the pupil of the microscope objective.

We acknowledge the financial support of ANR-TECSAN. We thank Charles Brossollet, Olivier de Witte and Bertrand de Poly for stimulating discussions.

## References

1. J. G. Fujimoto, M. E. Brezinski, G. J. Tearney, S. A. Boppart, B. E. Bouma, M. R. Hee, J. F. Southern, and E. A. Swanson, Optical biopsy and imaging using optical coherence tomography, *Nature Med.* 1, 970-972 (1995).  
A. F. Fercher, Optical coherence tomography, *J. Biomed. Opt.* 1, 157-173 (1996).  
G. J. Tearney, B. E. Bouma, S. A. Boppart, B. Golubovic, E. A. Swanson, J. G. Fujimoto *Opt. Lett.* 21, 1408-1410 (1996).
2. A. Dubois, L. Vabre, A.C. Boccara, and E. Beaurepaire, High-resolution full-field optical coherence tomography with a Linnik microscope, *Appl. Opt.* 41, 805-812 (2002).  
L. Vabre, A. Dubois, A.C. Boccara, Thermal-light full-field optical coherence tomography, *Opt. Lett.* 27, 530-533 (2002).
3. D. Debarre, M. J. Booth, and T. Wilson, Image based adaptive optics through optimisation of low spatial frequencies. *Optics Express* (2007) vol. 15 (13) pp. 8176-8190

4. Tearney et al. Determination of the refractive-index of highly scattering human tissue by optical coherence tomography. Optics Letters (1995) vol. 20 (21) pp. 2258-2260
5. Markus Rueckel, Julia A. Mack-Bucher, and Winfried Denk PNAS November 14, 2006 vol. 103 , no. 46 17137-17142